

Influence of various oxides on the complex network structure at high temperature condition

understanding of polymerization process of oxides

Jongbae, Kim
Research Institute of Steel
Yonsei Univ.
Seoul, Rep. of Korea
sszombie@nate.com

Il Sohn
Materials Science and Engineering
Yonsei Univ.
Seoul, Rep. of Korea
ilsohn@yonsei.ac.kr

Abstract—The influence of $\text{TiO}_2/\text{SiO}_2$ and $\text{SiO}_2/\text{Al}_2\text{O}_3$ ratio were verified to identify the individual function in construct of complex network structure and to examine the structural change at high temperature. The viscosity at high temperature decreased as $\text{TiO}_2/\text{SiO}_2$ ratio increased and increased as $\text{SiO}_2/\text{Al}_2\text{O}_3$ ratio increase at high temperature. The network structure was studied using Fourier transform infrared (FTIR) and X-ray Photoelectron spectroscopy (XPS). The $[\text{SiO}_4]^{4-}$ -tetrahedral symmetric stretching vibration and the $[\text{AlO}_4]^{5-}$ -tetrahedral asymmetric stretching vibration became less pronounced as $\text{TiO}_2/\text{SiO}_2$ ratio increase and the reverse phenomenon was observed as $\text{SiO}_2/\text{Al}_2\text{O}_3$ increase. XPS analysis also suggested that the network structure, which is constructed by dominant structural units, can be exchanged as bridged oxygen (O^0), non-birdged oxygen (O^\bullet) and free oxygen (O^{2-}) fractions. The activation energy for present slag system was calculated with Arrhenius type relationship equation.

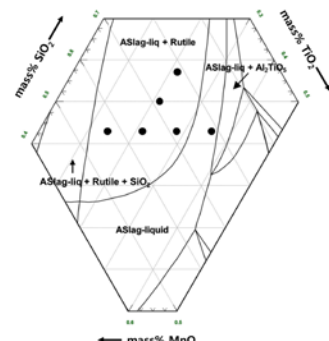
Keywords—viscosity; structure analysis; XPS; FTIR

I. INTRODUCTION

Recently, researchers have been increasingly giving an effort to improve the quality of steel due to the rising demand for high strength steel. One of the important steps to get improved steel is welding process. The stringent safety around welded area and the control of various impurities at the interface are necessary to materialize the welding zone. Furthermore, the contamination from the atmosphere determinates the welded steel properties.[1-3] Thus, the study on the fundamental relationship between welding flux and base metal and the additional understanding in phenomenon during welding procedure has to be accompanied in development.

In the aspect of designing of welding flux, it is so important to understand the characteristic flux properties such as viscosity, wettability and electric conductivity. Especially the viscosity significantly affects the wettability and crystallization phenomenon which can be directly connected with diffusion

coefficient. But the papers regarding the viscosity property and the effect of individual oxides on the network structure at high temperature including TiO_2 , MnO and Al_2O_3 contents have yet been broadly published up to the present. Amphoteric oxides TiO_2 , MnO and Al_2O_3 can act as both the network forming unit with supplied free oxygen (O^{2-}) and the network modifying unit which construct the network structure and increase the



viscosity such as SiO_2 .[4-8] So, the further study on TiO_2 , MnO , SiO_2 , Al_2O_3 and each function in network structure should be further discussed. In addition, both of Al_2O_3 and SiO_2 presence in slag system can increase the alumino-silicate structure, which can influence the thermodynamic property such as viscosity and spreading ability of flux.[9] Thus, in this study, the effect of $\text{TiO}_2/\text{SiO}_2$ ratio and the effect of Al_2O_3 substitution by SiO_2 in TiO_2 , MnO containing slag system were investigated.

Fig. 1. The experimental composition of TiO_2 - 30MnO - SiO_2 - Al_2O_3 based phase diagram calculated by FactSage®.

II. EXPERIMENT

A. sample preparation

All samples were prepared as the master slag of at least 160g by melting it at 1773K (1500°C) for 5 hours under 2 L/min of UHP Ar (99.9999vol%) using a resistance box furnace to achieve the homogeneity in every fragment composition. After viscosity measurement, all samples were analyzed with X-ray fluorescence (XRF, S4 Explorer; Bruker AXS GmbH Karlsruhe, Germany) to identify the composition changes between weighed and post-experimental compositions. XRF results were presented in **Table. 1**. From the XRF as the Al_2TiO_5 phase. The effect of the primary phase will be explained in the results session.

No.	1	2	3	4	5	6
Pre-experimental (weighed composition)						
TiO_2	40	35	30	30	30	30
MnO	30	30	30	30	30	30
SiO_2	15	20	25	20	15	30
Al_2O_3	15	15	15	20	25	10
Extended basicity	2.33	1.86	1.5	1.5	1.5	1.5
Post-experimental (XRF analysis)						
TiO_2	39.4	34	29.9	30.6	31	27.8
MnO	29.7	29.3	29.4	29.4	30.6	32
SiO_2	15.7	20.5	25.2	20.1	15.2	29.6
Al_2O_3	14.9	16	15.4	19.8	23	10.5
Extended basicity	2.26	1.73	1.46	1.5	1.61	1.49
$\text{TiO}_2/\text{SiO}_2$	2.5	1.65	1.19	1.53	2.03	0.94
$\text{SiO}_2/\text{Al}_2\text{O}_3$	1.05	1.28	1.64	1.02	0.66	2.82
Liquidus Temp. ($T_{\text{liq.}}:\text{K}$)	1720.1	1735.9	1745.6	1690.7	1719.2	1707.5

analysis, the negligible change was observed ensuring that there is no volatile element in the present oxide system. The compositions of the samples were also planned in advance using commercial program Factsage® calculation to predict whether the chosen composition would be melted at the experimental temperature range. The phase diagram of TiO_2 -30MnO-SiO₂-Al₂O₃ at 1673K (1400°C) was presented in **Fig. 1**, which shows the possible primary phases in the target temperature and the equilibrium condition. The expected primary phase was revealed as the TiO_2 (rutile) phase except for the one composition of the 30TiO₂-30MnO-15SiO₂-25Al₂O₃ slag system, where the primary phase was calculated

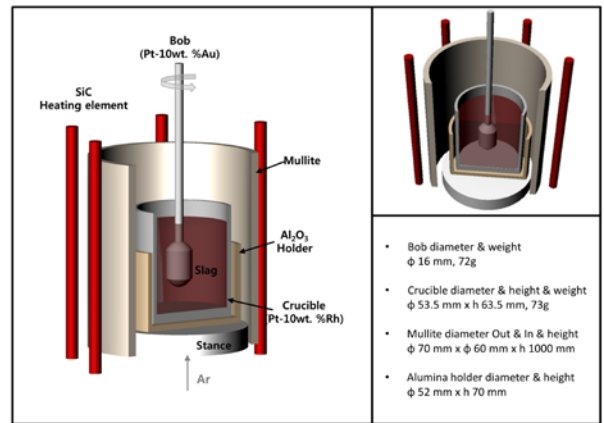


Fig. 2. The experimental apparatus & description.

TABLE I. PRE- AND POST-EXPERIMENTAL RESULTS FROM THE XRF ANALYSIS FOR THE TiO_2 -MNO-SiO₂-Al₂O₃ SLAG SYSTEM.

B. Viscosity measurements

The experimental conditions and the schematic of the experimental apparatus were presented in **Fig. 2**. The total of 120g master slag was put into the beaker type Pt-10Rh crucible and heated up to 1773K (1500°C) for 10 hours under the Ar 1L/min atmosphere in vertical resistance furnace. After the temperature was held for 3 hours for the sample to reach the thermal equilibrium and to be completely melted, the bob (Pt-10Rh) was inserted in the slag and the viscosity was conducted with commercial program measurement of Wingather 2.5version (Brookfield engineering laboratories, INC.). The Ar gas was refined with CaSO₄ and CaO vertical cylinder, which were directly connected with Ar gas barrel, to eliminate the excess moisture and CO₂ gas. The hot zone in vertical mullite furnace was identified as approximately 5cm to prevent the temperature gradient in all area and calibrated with a B-type reference thermocouple (Pt-10Rh). The temperature was controlled using a proportional-integral-derivative controller (PID) within $\pm 3\text{K}$ error. The viscosity values were measured using the Brookfield digital rheometer (LVDV-II+ ; Brookfield Engineering Laboratories, Middleboro, MA), which is

appropriate to measure an expected viscosity value range which was previously expected using Factsage[®] calculation, with 25K interval until more below than break temperature range (T_{br}). Each target temperature has been held for 15 min to reach an equilibrium state and held for 15 min for viscosity measuring process. All viscosity values were transformed from the torque to the Pa·s using standard silicon oil calibration.

C. Slag structure analysis using FTIR and XPS

The molten slag, after the viscosity measurements was quenched on a Cu mold which floated upon the liquid nitrogen to get a non-crystalline phase and analyze the complex network structure at 1773K (1500°C) with FTIR (Spectra100; Perkin-Elmer, Shelton CT, USA) and XPS (K-Alpha; Thermo Scientific Instrument, XPS mono, model : K-alpha by Thermo U. K.) assuming that the liquidus slag structure was maintained during quecnching. The O_{1s} XPS spectrum was measured using a monochromatic Al K α source and calibrated with the C1s core level standard at 285eV. After the base line was plotted with Shirley's method, the oxygen peak was deconvoluted and fitted as three type spectra such as free oxygen (O²⁻), non-bridged oxygen (O⁻), bridged oxygen (O⁰) using a mixed Gaussian-Lorentz function. The commercial software SDP v4.11 (XPS International, LLC software, USA) was chosen for deconvoluting of spectra. The three oxygen peaks with r^2 of over 0.99 were selected and fitted with a full-width half maximum (FWHM) of less than 2.0eV to ensure reliability which is presented in **Table 2**.

TABLE II. O_{1s} DECONVOLUTED PEAKS WITH EACH BINDING ENERGY(EV) AND FWHM(EV).

No.	(T+M)/(S+A)	SiO ₂ /Al ₂ O ₃	O ²⁻	FWHM	O ⁻	FWHM	O ⁰	FWHM
1	2.33	1.00	530.25	1.74	531.33	1.33	532.15	1.54
2	1.86	1.33	530.45	1.79	531.34	1.26	532.24	1.36
3	1.50	1.67	530.52	1.68	531.34	1.08	532.01	1.17
4	1.50	1.00	530.47	1.62	531.52	1.33	532.47	1.38
5	1.50	0.60	530.48	1.97	531.49	1.42	532.06	1.40
6	1.50	3.00	530.65	1.75	531.37	1.31	532.05	1.45

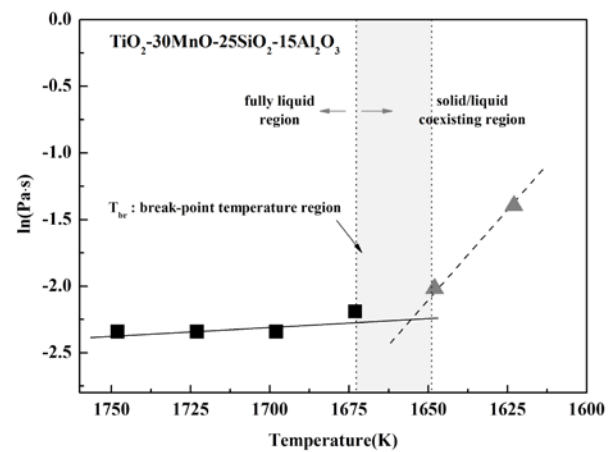


Fig. 3. Viscosity measurements of the fully liquid region and solid/liquid coexisting region beyond the break-point temperature in the 30TiO₂-30MnO-25SiO₂-15Al₂O₃ slag.

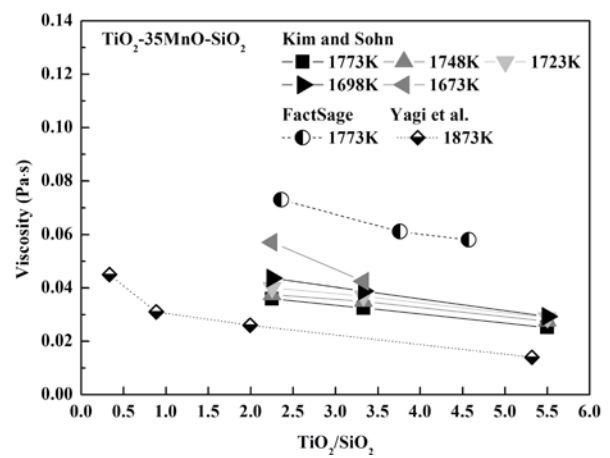


Fig. 4. Influence of TiO₂/SiO₂ ratio on the viscosity in the TiO₂-35MnO-SiO₂[10]

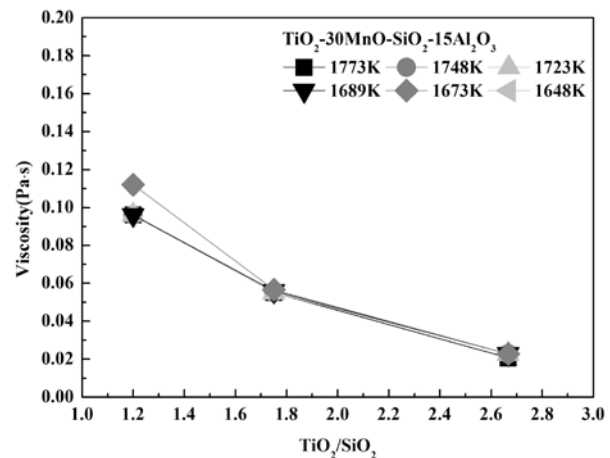


Fig. 5. Influence of TiO₂/SiO₂ ratio on the viscosity in the TiO₂-30MnO-SiO₂-Al₂O₃

III. RESULT AND DISCUSSION

A. Influence of TiO_2/SiO_2 and SiO_2/Al_2O_3 ratio on the viscosity

A primary phase appeared in liquid phase. Which temperature point usually called break temperature and it distinguished the fully liquid and liquid-solid coexisting temperature. But the exact break temperature can't be found during experiment thus, it can be expressed as break temperature range presented in **Fig. 3**.

Fig. 4 shows the influence of TiO_2/SiO_2 on the viscous behavior in the TiO_2 -MnO-SiO₂ slag system at various temperatures, the results of which were already discussed in the previous work which was published by Kim and Sohn[10] to identify how TiO_2 , MnO affects the silicate network structure is presented to compare between the ternary slag system. **Fig. 5** shows the influence of TiO_2/SiO_2 ratio on the viscous behavior of the TiO_2 -30MnO-SiO₂-15Al₂O₃ system. Both graphs present the viscosity values in the fully liquid region above break temperature region. As TiO_2/SiO_2 ratio increased, the similar trend was identified, where the viscosity values decreased linearly with TiO_2/SiO_2 ratio increase. The amphoteric oxide Al₂O₃ seems to make the viscosity increase and steeper with TiO_2/SiO_2 ratio variation and work as acidic oxide promoting the formation of the complex silicate structure. It can be understood that the excessive TiO_2 and MnO content result in the lower viscosity values in individual way. This will be further discussed in structural analysis part. It can be expected that the measured viscosity values in the present quaternary TiO_2 -MnO-SiO₂-Al₂O₃ slag system at high temperature region relatively higher than the ternary TiO_2 -MnO-SiO₂ slag system when the TiO_2/SiO_2 ratio is lower than 2.0 according to the slopes of the viscosity values. This expectation could be reconfirmed from the Factsage® calculation between TiO_2/SiO_2 ratio of 2.0 and 0.8 in **Fig. 4**. **Fig. 6** shows the viscosity variation with another reference, Saito et al., which a function of extended basicity. The definition of extended basicity can be expressed as the summation of basic oxides over the summation of acidic oxides. Thus, the extended basicity by Saito et al.[11] results can be defined as $(TiO_2+CaO)/(SiO_2+Al_2O_3)$. It usually presents the comparable effect of oxides in the composition variation included various oxides. Both results show the similar viscosity with the extended basicity. The viscosity trend between 1773K ($1500^{\circ}C$) from the 1673K ($1400^{\circ}C$) shows almost the same values but the viscosity values near the break temperature region seems to be off the linear trend. The results by Saito et al. seem to converge at an extended basicity around 1.0 and the slope is steeper than the slope in the present slag system TiO_2 -MnO-SiO₂-Al₂O₃. This can be speculated that the influence of the basic oxides on the network structure is different and it depends on how efficiently the large network structure is depolymerized with the addition of basic oxide such as MnO and CaO contents. **Fig. 7** shows the effect of Al₂O₃ substitution by SiO₂ on the viscous behavior at high temperature. The viscosity in the high temperature range between from 1773K ($1500^{\circ}C$) to 1723K ($1450^{\circ}C$) seems to be leveled out with SiO_2/Al_2O_3 ratio increase and consequentially saturated at

SiO_2/Al_2O_3 of 3.0. The primary phase difference, which was calculated by Factsage®, results in the significant change on the viscous property at high temperature. At SiO_2/Al_2O_3 of below 1.0, the primary phase was revealed as Al₂O₃-TiO₂ phase and TiO₂ rutile phase above 1.0. It can also be understood that the Al₂O₃-TiO₂ primary phase was performed at SiO_2/Al_2O_3 of 0.6 under the equilibrium cooling conditions and the TiO₂ rutile phase was performed in other SiO_2/Al_2O_3 conditions. Little viscosity change was observed and the temperature dependence was insignificant in all compositions

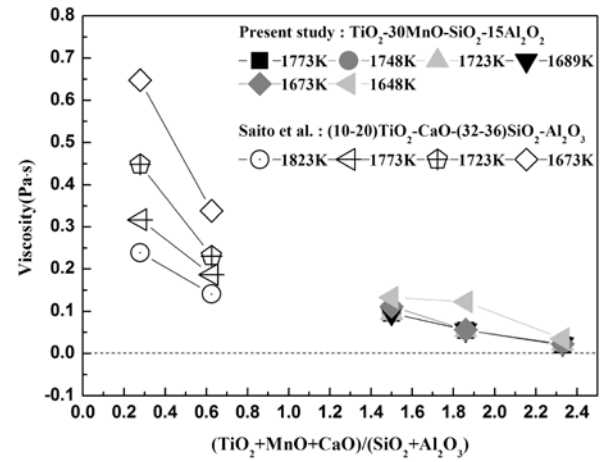


Fig. 6. Influence of extended basicity on the viscosity of the TiO_2 -MnO-SiO₂-Al₂O₃ and TiO_2 -CaO-SiO₂-Al₂O₃ slag system.

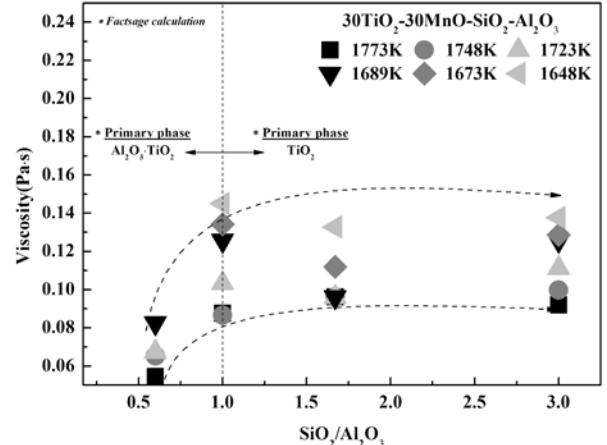


Fig. 7. Influence of SiO_2/Al_2O_3 ratio on viscosity in TiO_2 -MnO-SiO₂-Al₂O₃ slag system.

B. FTIR, XPS structural analysis

Fig. 8 shows FTIR troughs with transmittance from $400cm^{-1}$ to $1300cm^{-1}$ providing the degree of polymerization in the TiO_2 -30MnO-SiO₂-15Al₂O₃ slag system at various TiO_2/SiO_2 ratios. It also presents the structural status of the bonding characteristics of the molten slag. The vibration region from $850cm^{-1}$ to $1200cm^{-1}$ was identified as the $[SiO_4]^{4-}$ -tetrahedral symmetric stretching vibration[12] and the one from $600cm^{-1}$ to $800cm^{-1}$ was identified as the $[AlO_4]^{5-}$ -tetrahedral

asymmetric stretching vibration.[13] According to Haung et al.[14], the characteristic vibration around 450cm^{-1} corresponds to the Al-O-Si bending vibration. The $[\text{SiO}_4]^{4-}$ -tetrahedral symmetric stretching vibration was significantly less pronounced with $\text{TiO}_2/\text{SiO}_2$ ratio increase and it can be considered as the absolute concentration of SiO_2 content became lower but the $[\text{AlO}_4]^{5-}$ -tetrahedral asymmetric stretching vibration and Si-O-Al bending vibration were relatively unaffected with $\text{TiO}_2/\text{SiO}_2$ ratio variation. **Fig. 9** shows the influence of $\text{SiO}_2/\text{Al}_2\text{O}_3$ ratio on the alumina-silicate based network structure at extended basicity of 1.5. The $[\text{SiO}_4]^{4-}$ -tetrahedral symmetric stretching vibration and the $[\text{AlO}_4]^{5-}$ -tetrahedral asymmetric stretching vibration seem to be pronounced with higher $\text{SiO}_2/\text{Al}_2\text{O}_3$ ratio but the Al-O-Si bending vibration seems to be distinguished from the standard point at $\text{SiO}_2/\text{Al}_2\text{O}_3$ of 1.67. If the higher $\text{SiO}_2/\text{Al}_2\text{O}_3$ ratio than 1.67, Al-O-Si bending vibration decreased and it is caused where the alumina-silicate network structure is strongest at $\text{SiO}_2/\text{Al}_2\text{O}_3$ ratio 1.67 and the dominant network structure was divided as two cases. **Fig. 10** and **Fig. 11** describe the function of the bridged oxygen (O^0), non-bridged oxygen (O^-) and free oxygen (O^{2-}) as a function of $\text{TiO}_2/\text{SiO}_2$ and $\text{SiO}_2/\text{Al}_2\text{O}_3$ ratio. As a result of depolymerization process, the previous paper by Toop and Samis suggest following equation.[15]



Each bridged oxygen (O^0) and free oxygen (O^{2-}) is transformed to the two non-bridged oxygen (O^-). The non-bridged oxygen (O^-) can be understood as the degree of depolymerization in network structure which is constructed by only oxides. When $\text{TiO}_2/\text{SiO}_2$ ratio increased, the bridged oxygen (O^0) and the free oxygen (O^{2-}) factors were slightly decreased which seems to be caused as the TiO_2 contents didn't work as the basic oxide such as CaO , MnO , which depolymerizes the network structure at high temperature but TiO_2 content seems to be existed with own structure. According to Mysen, The Ti-O-Ti stretching vibration has to be detected around 830cm^{-1} , If TiO_2 content polymerized the networking structure but it wasn't detected in present slag system. Furthermore, According to Yagi et al.,[10] he suggested the TiO_2 dilution effect and SiO_2 substitutional effect on the complex silicate structure and viscous behavior as decrease. The phenomenon of the little decrease of non-bridged oxygen (O^-) and little increase of bridged oxygen (O^0), free oxygen (O^{2-}) were identified from the **Fig. 11** but the different phenomenon as $\text{TiO}_2/\text{SiO}_2$ in **Fig. 10**. It isn't also presented significant changes with higher $\text{SiO}_2/\text{Al}_2\text{O}_3$. According to Mysen and Richet,[16] Ti-O-Al vibration and Ti-O vibration can make the short rang ordered simple oligomer structures in a melts and decrease the viscosity behavior. The both $[\text{SiO}_4]^{4-}$ -tetrahedral symmetric stretching vibration and the $[\text{AlO}_4]^{5-}$ -tetrahedral asymmetric stretching vibration weren't significant below the $\text{SiO}_2/\text{Al}_2\text{O}_3$ ratio of 1.67. It seems to be caused with the absence of complex structural units such as silicate or aluminate but the presence of the simple structural units such as Ti-O-Al structure. In addition, the characteristic vibration of Ti-O-Al suggested by Saito et al. should be found in near 583cm^{-1} and 439cm^{-1} with low intensity, but these also not observed in $30\text{TiO}_2\text{-}30\text{MnO}\text{-}\text{SiO}_2\text{-}\text{Al}_2\text{O}_3$ slag system from the FTIR analysis in **Fig. 9**. Above the $\text{SiO}_2/\text{Al}_2\text{O}_3$ ratio of 1.67,

the silicate tetrahedral structure was polymerized with SiO_2 concentration increase, where the $[\text{SiO}_4]^{4-}$ -tetrahedral symmetric stretching vibration has shown the noticeable intensity increase.

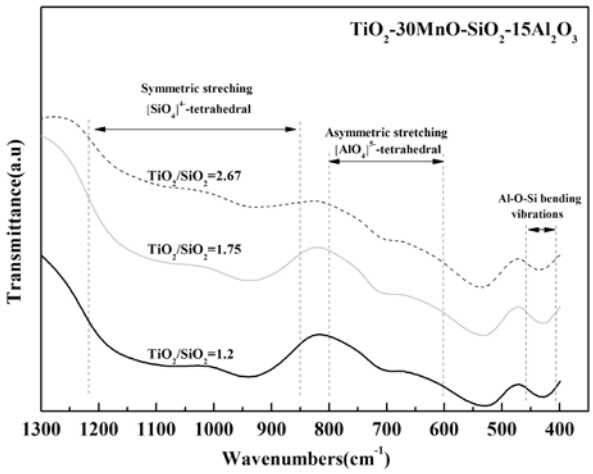


Fig. 8. Influence of $\text{TiO}_2/\text{SiO}_2$ on the network structure at fixed MnO , Al_2O_3 contents by FTIR analysis of as-quenched slag at 1773K.

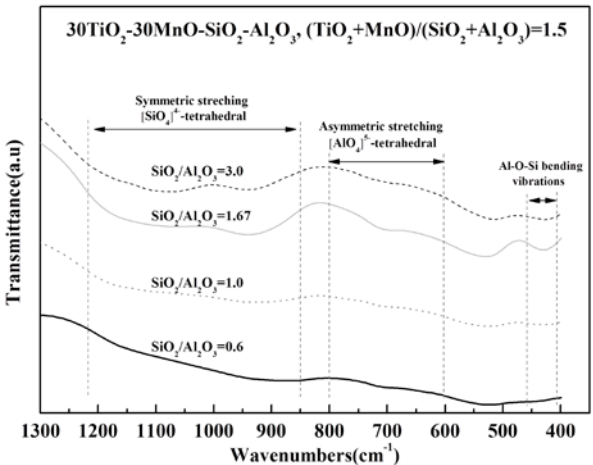


Fig. 9. Influence of $\text{SiO}_2/\text{Al}_2\text{O}_3$ on the network structure at fixed $(\text{TiO}_2+\text{MnO})/(\text{SiO}_2+\text{Al}_2\text{O}_3)$ of 1.5 by FTIR of as-quenched slag at 1773K.

C. The temeprature dependance

Fig. 12 shows the influence of $\text{TiO}_2/\text{SiO}_2$ and $\text{SiO}_2/\text{Al}_2\text{O}_3$ ratios on the activation energy, which calculated with Arrhenius type relationship equation. The activation energy informs how much large gradient of the viscosity values was occurred in specific composition during temperature decrease because the slope of reciprocal temperature over the measured viscosity values is used for the calculation to fine the each activation energies of various compositions. The comparable temperature dependency of the viscosity with $\text{TiO}_2/\text{SiO}_2$ and $\text{SiO}_2/\text{Al}_2\text{O}_3$ ratios in present slag system was identified. The apparent activation energy on $\text{TiO}_2\text{-}30\text{MnO}\text{-}\text{SiO}_2\text{-}15\text{Al}_2\text{O}_3$ system with various $\text{TiO}_2/\text{SiO}_2$ ratios was calculated from

30.48 to 6.41 kJ/mol, which is extremely low depolymerized energy. This can be caused by the presence of TiO_2 content with high concentrations. Previous paper by researches suggested the low temperature dependency of TiO_2 dominant slag system. However, the activation energy trend isn't unclear in **Fig. 12 (a)** because the error bars with large range are existed. Thus, it can't be defined as whether the activation energy decreased with higher $\text{TiO}_2/\text{SiO}_2$ ratio or stable with extremely low energy. The activation variation in **Fig. 12 (b)** seems to be correlated well with viscosity trend, which was explained in viscosity and structure analysis parts. The existence of Ti-O-Al simple structure makes the activation energy higher below $\text{SiO}_2/\text{Al}_2\text{O}_3$ ratio of 1.67. The activation energy, which was calculated from 128.03 to 30.48 kJ/mol, also rose above $\text{SiO}_2/\text{Al}_2\text{O}_3$ ratio of 1.67 with complex silicate network structure increase.

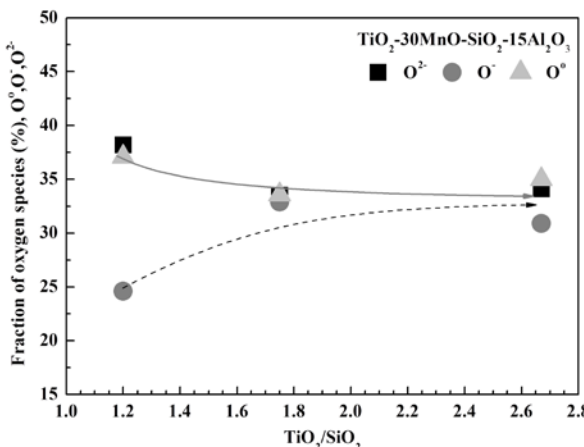


Fig. 10. Influence of $\text{TiO}_2/\text{SiO}_2$ on the network structure at fixed MnO , Al_2O_3 contents by XPS of as-quenched slag at 1773K

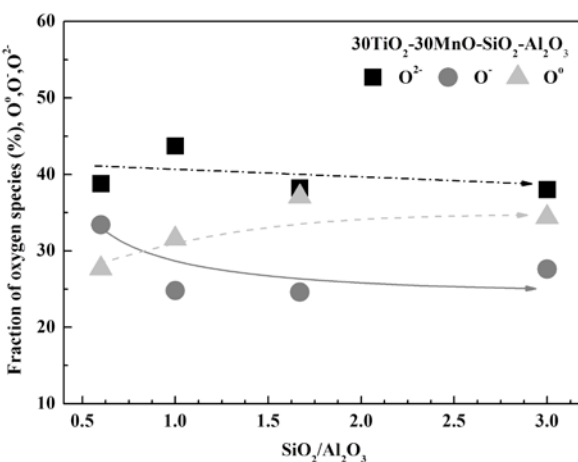


Fig. 11. Influence of $\text{SiO}_2/\text{Al}_2\text{O}_3$ on the network structure at fixed TiO_2 , MnO contents by XPS of as-quenched slag at 1773K .

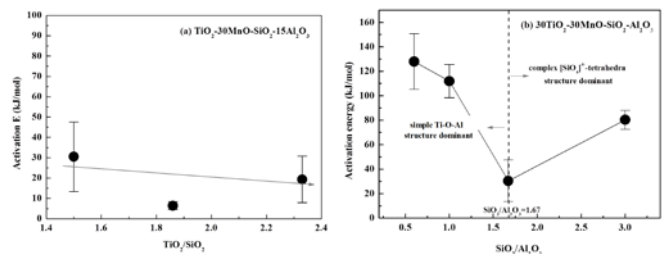


Fig. 12. The activation energy by using Arrhenius type relationship calculation in $\text{TiO}_2\text{-MnO-SiO}_2\text{-Al}_2\text{O}_3$ slag system.

The influence of $\text{TiO}_2/\text{SiO}_2$ and $\text{SiO}_2/\text{Al}_2\text{O}_3$ ratios was identified with $\text{TiO}_2\text{-MnO-SiO}_2\text{-Al}_2\text{O}_3$ slag system. The viscous behavior was affected by the primary phases at high temperature region. The simple structure of TiO_2 was substitutes the complex networks structure of $[\text{SiO}_4]^{4-}$ -tetrahedron, which caused decrease of viscosity at $\text{TiO}_2\text{-30MnO-SiO}_2\text{-15Al}_2\text{O}_3$ slag system. When Al_2O_3 content substituted with SiO_2 content, the viscosity linearly increased until it saturated around $0.1\text{Pa}\cdot\text{s}$. This phenomenon seems to be induced by the primary phase difference and the dominant network structure change, which was divided with standard at $\text{SiO}_2/\text{Al}_2\text{O}_3$ of 1.67. It is reasonable that the $[\text{SiO}_4]^{4-}$ -tetrahedral structure was dominant over $\text{SiO}_2/\text{Al}_2\text{O}_3$ ratio of 1.67 and Ti-O-Al structure was dominant below $\text{SiO}_2/\text{Al}_2\text{O}_3$ ratio of 1.67. The structure analysis was supported by XPS deconvoluted results. The apparent activation energy was calculated by Arrhenius type relationship equation and the slope of the viscosity values within the fully liquid region as between 19.29 and 128.03 kJ/mol.

REFERENCES

- [1] A. Joarder, S.C. Saha, and A.K. Ghose : Weld.J. Res. Suppl., 70 (1991), 141.
- [2] T.W. Eagar : Weld.J. Res. Suppl, 57 (1978), 76.
- [3] C.S. Chai and T.W. Eagar : Weld.J. Res. Suppl 16 (1982), 229.
- [4] H. S. Park, J. Y. Park, G. H. Kim, and I. Sohn : Steel Res. Int., 83 (2012), 150.
- [5] S. M. Jung and R. J. Fruehan : ISIJ Int., 41 (2001), 1447.
- [6] Xie, D., Y. Mao, and Y. Zhu. : J. S. Afr. Inst. Min. Metall., 25. (2004) 43.
- [7] B. O. Mysen : Am. Mineral., 65 (1980), 1150.
- [8] J. O. M. Bockris, and D. L. Lowe : Proc. R. Soc. London, Ser. A, 226 (1954) 423.
- [9] G. Kim, and I. Sohn : ISIJ Int., 52 (2012) 68.
- [10] J. B. Kim and I. Sohn: J. Non-Cryst. Solid, 379 (2013), 235.
- [11] N. Saito, N. Hori, K. Knakshima, and K. Mori ; MMTB, 34B (2003), 509.
- [12] D.W. Matson, S.K. Sharma, and J.A. Philpotts : J. Non-Cryst.Solids, 58 (1983), 323.
- [13] M. Persson, and S. Seetharaman : ISIJ Int., 47 (2007), 1771
- [14] C. Huang, and E.C. Behrman : J. Non-Cryst.Solids, 128 (1991), 310.
- [15] G.W. Toop, C. S. samis : Trans. AIME., 224 (1962). 870.
- [16] B. O. Mysen, and P. Richet : Silicate glasses and melts (properties and structure), 2005, elsevier developments in geochemistry 10.